Theor Appl Climatol (2012) 109:245–252
DOI 10.1007/s00704-011-0580-z

ORIGINAL PAPER

Transient response to well-mixed greenhouse gas changes

Isabella Bordi · Klaus Fraedrich · Alfonso Sutera · Xiuhua Zhu

Received: 7 July 2011 / Accepted: 22 December 2011 / Published online: 10 January 2012

Abstract A change in CO_2 concentration induces a direct radiative forcing that modifies the planetary thermodynamic state, and hence the surface temperature. The infrared cooling, by assuming a constant temperature lapse-rate during the process, will be related to the surface temperature through the Stefan–Boltzmann law in a ratio proportional to the new infrared opacity. Other indirect effects, such as the water vapor and ice-albedo feedbacks, may amplify the system response. In the present paper, we address the question of how a global climate model with a mixed layer ocean responds to different rates of change of a well-mixed greenhouse gas such as CO_2. We provide evidence that different rates of CO_2 variation may lead to similar transient climates characterized by the same global mean surface temperature but different values of CO_2 concentration. Moreover, it is shown that, far from the bifurcation points, the model's climate depends on the history of the radiative forcing displaying a hysteresis cycle that is neither static nor dynamical, but is related to the memory response of the model. Results are supported by the solutions of a zero-dimensional energy balance model.

1 Introduction

The response of a physical system to an external time-dependent forcing depends on the rate on which the forcing is applied, and on the time scale on which the system relaxes to its equilibrium. If the latter time scale is very short compared to the rate of change of the forcing (i.e., the forcing varies adiabatically), the relationship between response and forcing can be easily computed by considering the steady solutions as a function of the forcing parameter. This does not hold when the system is nonlinear and its relaxation time scale is of the same order as the one of the forcing change or longer. In such a case, the system is not able to relax completely to the new equilibrium and what is observed is the transient response to the time-dependent forcing that will be driven by the memory of the system. Climate is a physical system where these issues need to be addressed. An example is given by the study of the climate (transient) response to a well-mixed greenhouse gas like CO_2 that varies at a given time rate, which is the topic of the present paper.

Manabe et al. (1991) carried out experiments with a comprehensive climate model where the CO_2 concentration was increased or decreased with respect to a nominal value at the same time rate. They found an almost symmetric response, i.e., the geographical distribution of the air surface temperature reduction in the CO_2 decrease experiment was similar to the distribution of the warming in the CO_2 growth experiment. Held et al. (2010), on the other hand, described the response of the GFDL CM2.1 model when, along the trajectory of the model forced by an increasing CO_2 concentration, a sudden return to the preindustrial value is imposed. They found that there were two components of the system response: the fast one equilibrates with the sudden perturbation, while the other is sluggish, so that the model appeared to be "recalcitrant" to reach equilibrium. This slow component may suggest that the full response departs from the symmetry envisioned in the Manabe et al. (1991) experiment, and a more complex behavior might

I. Bordi (✉) · A. Sutera
Department of Physics, Sapienza University of Rome,
Rome, Italy
e-mail: isabella.bordi@roma1.infn.it

K. Fraedrich · X. Zhu
KlimaCampus, Universität Hamburg,
Hamburg, Germany

occur. For example, if we measure the thermodynamic state of the system through some metrics (say the global mean surface temperature as is usually done), a different transient climate may be achieved by the same forcing value, or the model trajectory would have hysteresis if the forcing is reversed at a given time.

In the present paper, to analyze these concepts, we consider a global climate model (GCM) briefly presented in the next section. The atmosphere, ocean, and sea ice interact through the usually stated physical laws, while the forcing is provided through the radiative imbalances induced by decreasing the atmospheric CO_2 concentration. In particular, after determining the equilibrium conditions for CO_2= 360 ppm, this concentration is linearly decreased up to 20 ppm with different time rates. The latter value is chosen because the GCM here considered is found to reach an ice-covered Earth state below this amount of CO_2 concentration. It is worth noting that a sudden variation of the CO_2 content from 360 to 20 ppm provides a change of about 10 Wm^{-2} in the outgoing thermal radiation (estimation based on the radiative transfer model MODTRAN (Berk et al. 1989) for the US Standard Atmosphere in clear sky conditions). However, simple sensitivity analyses do not justify the low temperatures observed in response to such a change of the radiative forcing, unless also water vapor changes substantially. It turns out that there is a strong water vapor feedback in the GCM, so that, for such a perturbation, cold surface temperatures are achieved and sea ice advances equatorward. Note that in this model, by reducing CO_2 content up to 20 ppm the induced change in the surface albedo is not enough to trigger the ice-albedo feedback at global scale.

The model response should clearly depend on the rate of CO_2 decrease. However, the concurrence of other effects might lead to a non-unique relationship between the climate change metric (usually the global mean surface temperature is used for its intuitive meaning) and the CO_2 atmospheric content. In this circumstance, as shown in the next section, the target value of the climate metric for a given CO_2 concentration may be, at the very least, an inconsistent appraisal of the climate system.

The present paper will also address the issue of whether the GCM shows hysteresis, namely if the model response moves along a different trajectory when the CO_2 content is first decreased at some rate and then reversed at the same rate. Recently, this aspect has been addressed for other forcing agents (variations in the solar constant, Lucarini et al. 2010, or in the oceanic salt gradient for the study of the thermohaline circulation, Rahmstorf 1995) but not for variations in the atmospheric CO_2 concentration. It is expected that hysteresis manifests in the model behavior. On one hand, there is a low critical value of CO_2 for which the model jumps to the ice-covered state and becomes rather insensitive to further decreases of the greenhouse gas. On the other hand, since the relationship between CO_2 concentration and radiative forcing is logarithmic, reasonable increased concentrations of this greenhouse gas have a progressively smaller warming effect. Between these two extreme conditions should be a range of the radiative forcing where multiple steady states co-exist (ice-free and ice-covered Earth state). Also, the presence of a slow component in the model response would imply a memory effect propagating forward in time. Generally speaking, a system with these properties might present hysteresis (i.e., multiple transient responses to a temporal reversal of forcing) and, as in Held et al. (2010), should possess a recalcitrant component.

2 A planet simulator analysis

Analyses are performed using the portable global climate model Planet Simulator (PlaSim, freely available under http://www.mi.uni-hamburg.de/plasim, Fraedrich et al. 2005). The model is a simplified yet Earth-like spectral model used here in a configuration of T21 horizontal resolution with 17 sigma levels in the vertical. The atmospheric component has been used (Bordi et al. 2007) to test a hypothesis on the baroclinic adjustment theory (Bordi et al. 2004). The ocean is represented by a 50-m slab ocean, which includes a zero-dimensional thermodynamic sea ice model (Fraedrich and Lunkeit 2008).

PlaSim is run with CO_2=360 ppm until it reaches equilibrium. From there on, the atmospheric CO_2 concentration is reduced at a constant time rate down to 20 ppm. Then, keeping the CO_2 content constant , the system is left to evolve towards the equilibrium associated with that radiative forcing. As reported in Fig. 1a, where the time behavior of the global annual mean surface temperature T_s is displayed, six different time rates are considered. The figure shows what may be expected by a relaxation system where the time rate varies with the CO_2 concentration from one run to the next. Also, the relaxation time towards the equilibrium ($T_s \approx 247$ K) appears to be a function of the time rate of CO_2 reduction rather than to be determined by the internal dynamics. At CO_2=20 ppm, the climate model reaches different temperatures that are as close to the equilibrium as the time rate is slower (almost adiabatic change of the radiative forcing). This is clearly evident from Fig. 1b where the global mean surface temperature as a function of CO_2 concentration is shown for each run. As will be discussed in the next section, these features characterizing the transient response of PlaSim are responsible of the model behavior when CO_2 concentration is increased back from 20 to 360 ppm. In fact, since the radiative forcing variation is faster than the time needed for the system to relax

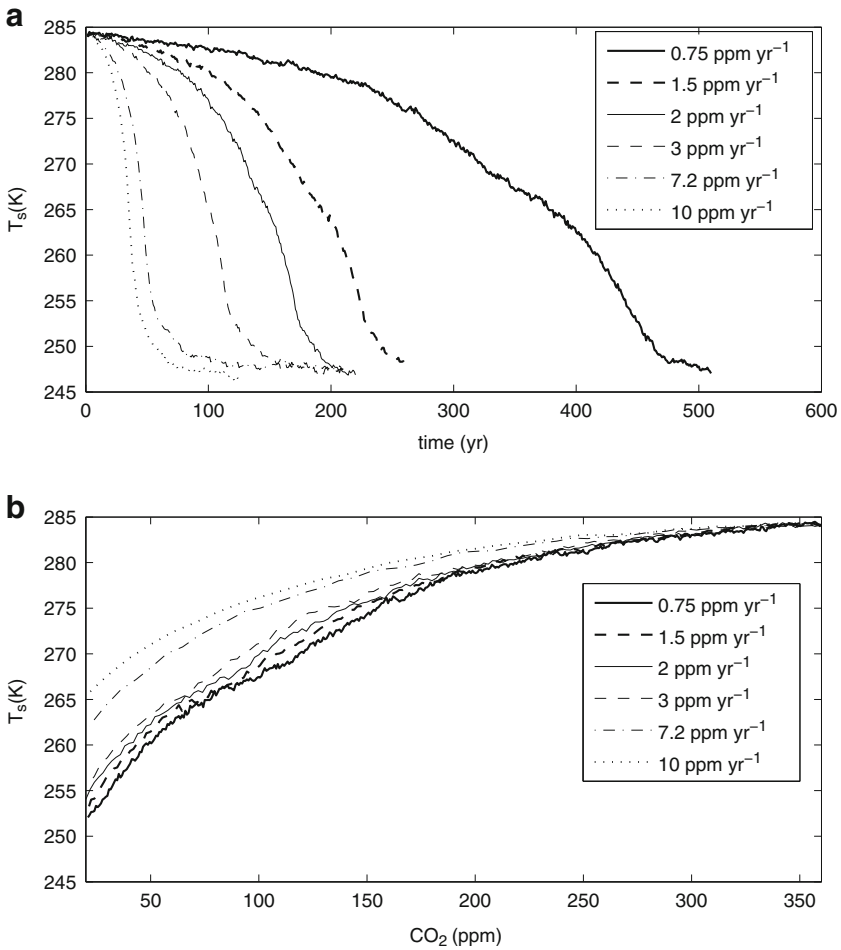

Fig. 1 Global mean surface temperature T_s (K) as a function of: **a** time (year) for six decreasing rates of CO_2 content (0.75, 1.5, 2, 3, 7.2, and 10 ppm year^{-1}); **b** CO_2 concentration (ppm) for the same decreasing rates. Values of the surface temperature are yearly means

completely to the equilibrium, it is expected that the model does not follow the same trajectory when the radiative forcing is increased (i.e., the model response will have hysteresis).

Another interesting feature that emerges from Fig. 1b is that the different rates of CO_2 change lead to similar transient climates characterized by the same global mean surface temperature but different values of CO_2 concentration. As an example, the average temperature of 273 K is obtained within a range of about 50 ppm from the fastest to the slowest rate of CO_2 change. This suggests caution in associating a target value of the climate metric, T_s, to a given CO_2 concentration.

3 Memory response

In this section, the response of a zero-dimensional energy balance model is studied with the outgoing infrared radiation changing cyclically between the extreme conditions of maximum and minimum greenhouse effect. The analysis is then restricted to the case for which the range of variation of the radiative forcing does not include the bifurcation points. Lastly, it is investigated if the response of PlaSim to cyclic changes of CO_2 concentration behaves likewise.

3.1 Zero-dimensional energy balance model

Let us consider the following simple ordinary differential equation as in Goldsztein et al. (1997; see also Freidlin and Mayergozy 2001):

$$\varepsilon \frac{dx}{dt} = x(1-x^2) + \widehat{E} \tag{1}$$

with $\widehat{E} = \sin(\omega t)$. In case $\omega \to 0$ and $\varepsilon << 1$, the forcing $\hat{E}$ varies extremely slowly (adiabatically) in the interval of its definition, and the plot $x(t)$ versus $\hat{E}$ tracks the curve of steady states showing a hysteresis loop that is usually called a *static hysteresis*. For $\omega > 0$ and $\hat{E}$ varying slowly but not adiabatically in the same range, a new hysteresis loop is obtained that is usually called a *dynamical hysteresis*. The quantity of relevance will be the difference of the area between the dynamical loop and the static one. It is a measure of the dynamical response of the system to the external forcing (note that now ε may be of order ω, and, therefore, cannot be neglected). Generally speaking, the area

of the dynamical loop is greater than the static loop and the limit for $\omega \to 0$ may be different from zero. As in any hysteresis cycle, it represents the work done by the non-conservative forces on the system. It is worth noting that the mechanism of stochastic resonance (Benzi et al. 1981) can change the turning points where the system jumps from one stable branch to the other, and can be interpreted as a static hysteresis with less area.

Now consider the simple time-dependent zero-dimensional energy balance model (EBM):

$$C\frac{d}{dt}T_s = Q(1-\alpha) - (1-\beta)(A + BT_s) \tag{2}$$

Here, t, C, T_s, Q, α and β are the time, the heat capacity, the surface temperature (in degree Celsius), the incoming solar radiation, the planetary albedo, and the greenhouse gas parameter, respectively; A and B are constants. We wish to describe the solution of this equation for $\beta \in [\beta_1, \beta_2; 1 > \beta_1 > \beta_2]$. Let the albedo be defined as the usual step function

$$\begin{cases} \alpha = 0.35 & T_s > -10\,\mathrm{C} \\ \alpha = 0.8 & T_s < -10\,\mathrm{C} \end{cases} \tag{3}$$

and β, which represents a radiative forcing parameter, is a function of time t that changes linearly at a rate a between the two boundary values β_1 and β_2 as

$$\begin{cases} \beta(t) = \beta_{01} - a\,t & \text{for } t \in [(n-1)\,\tau,\ n\tau], \quad n = 1,\ 3,\ 5,\ \ldots \\ \beta(t) = \beta_{02} + a\,(t-\tau) & \text{for } t \in [(m-1)\,\tau,\ m\tau], \quad m = 2,\ 4,\ 6,\ \ldots \end{cases} \tag{4}$$

with $\tau = (\beta_1 - \beta_2)/a$ the time needed to span a half cycle (from β_1 to β_2 or vice versa), while β_{01} and β_{02} are determined by the boundary conditions $\beta((n-1)\,\tau) = \beta_1$ and $\beta((m-1)\,\tau) = \beta_2$.

As in Budyko (1969), A=320 $\mathrm{Wm^{-2}}$, B=4.6 $\mathrm{Wm^{-2}\,K^{-1}}$ and Q=340 $\mathrm{Wm^{-2}}$.

Now, setting β_1=0.9 and β_2=0.1, the selected boundary values for β represent the extreme conditions of maximum greenhouse effect (almost all outgoing infrared radiation is trapped by the atmosphere) and of minimum greenhouse effect (when almost all the infrared radiation is emitted to space), respectively. If the heat capacity C is set to zero and β varies extremely slowly (adiabatically) back and forth in the selected interval, then the static hysteresis loop shown in Fig. 2a (dash-dotted curve) is obtained. For C=50 $\mathrm{Wm^{-2}\,K^{-1}}$ year and β varying back and forth in the same interval at the rate a=0.001 $\mathrm{year^{-1}}$, a dynamical hysteresis loop emerges (Fig. 2a, solid curve). Within the range of β variability, the values of the radiative forcing which lead to the transition from ice-free to ice-covered Earth state and vice versa can be easily estimated from the upper and lower branches of the hysteresis cycles. Note that by construction, such transitions occur when there is a change in the albedo α, i.e., the surface temperature crosses the threshold of −10°C. Also, it can be noted that the dynamical hysteresis shows different transition points compared to the static hysteresis.

Now, the interesting question is whether a dynamical hysteresis may be obtained even without bifurcation on the r.h.s. of the EBM. To illustrate this case, let consider $\beta \in [0.4, 0.21]$ so that the system is linear with $T_s > -10$°C and α = 0.35. It is worth noting that β_1=0.4 is an estimation of the greenhouse parameter proper for the present climate conditions (i.e., α= 0.35 and T_s=15°C); the value of β_2=0.21, instead, has been estimated from Fig. 2a as the lower boundary of β before transition to the ice-covered Earth state. For C=0, the solution of the EBM will follow the continuous set of steady states determined by the value of β at a given time without static hysteresis. For $C \neq 0$, instead, the solutions will depart from the steady states because of the delayed response of the system induced by the heat content (l.h.s. of the EBM). This departure is expected to be positive when β decreases and negative when β increases. Since the end points, β_1 and β_2, are fixed, the two branches will join there, so that the full cycle should follow a closed curve in the (β, T_s)-plane. Now let us call β the input, our equation the transducer, and T_s an observation, then the latter solution is a description of a dynamical hysteresis loop that has no static counterpart. Therefore, since such a loop cannot be described by the static or the dynamical hysteresis as discussed by Goldsztein et al. (1997) (in fact, it does not represent the locus of the steady states and it does not include the bifurcation points), we coin it *memory hysteresis*. This hysteresis loop is due to a kind of memory effect of the model: the system responds on a longer time scale with respect to that of the forcing change, so that the system has a time delay in adjusting itself to the time-dependent forcing variation. Moreover, for a given time rate of change of the radiative forcing parameter, the source of this memory effect lies in the heat capacity C of the system whose magnitude controls the width of the hysteresis loop. As for this case entropy is not a well-defined quantity, the area enclosed in the loop will not equal the entropy production. Instead, the area is a measure of the resilience and the memory of the model to the time-dependent change of the forcing greenhouse parameter.

As an example, the EBM solutions (T_s vs β) for a given time rate a and two values of the heat capacity C are shown in Fig. 2b. As anticipated, a hysteresis loop occurs. The dash-dotted curve is the locus of the model steady states, while the time-dependent solutions for decreasing (increasing) β are shown for large (dashed) and small (full) heat capacities. At least three features are worth to be mentioned. First, we may get the same temperature for different greenhouse gas parameters. Second, when the model switches from decreasing to increasing β, and vice versa, the model response lags the forcing so that the surface temperature will continue to increase (or decrease) despite the fact that the

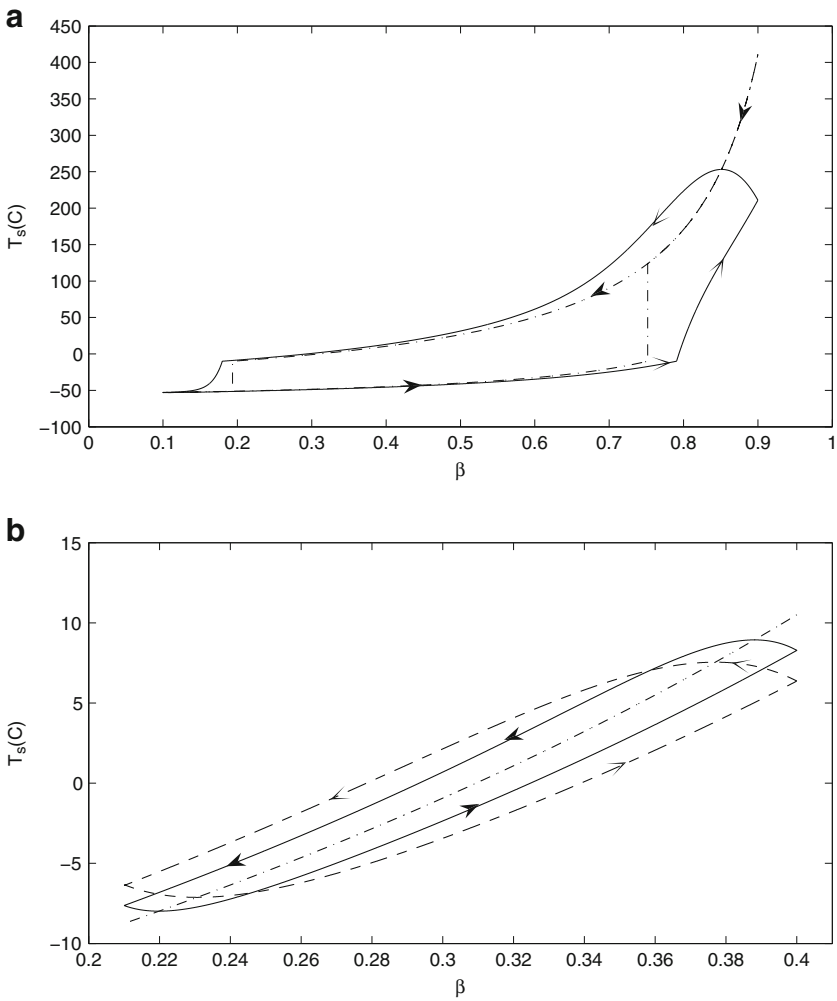

Fig. 2 EBM solutions in (β, T_s)-plane: **a** static hysteresis loop (*dash-dotted line*) for C=0 and β varying statically back and forth in the interval [0.9, 0.1], and dynamical hysteresis loop (*solid line*) for C= 50 Wm^{-2} K^{-1} year and β varying in the same interval at the rate a=0.001 $year^{-1}$; **b** locus of steady states (*dash-dotted line*) for C=0 and β varying statically in the interval [0.4, 0.21], and memory hysteresis loops for C=50 Wm^{-2} K^{-1} year (*solid line*), C= 100 Wm^{-2} K^{-1} year (*dashed line*) and β varying in the same interval at the rate a= 0.001 $year^{-1}$. Units are dimensionless and in degree Celsius for T_s and β, respectively

forcing is already decreasing (or increasing). Third, an increasing heat capacity C enhances the effect of the system's memory broadening the memory hysteresis loop. Furthermore, the lagged response found here is not easily associated with the recalcitrant or slow response discussed by Held et al. (2010), though it has a similar effect. The slow component of the global warming isolated by Held et al. (2010) refers to the climate model response towards equilibrium to an instantaneous return to the preindustrial radiative forcing. In that study, two heat capacities are considered in the EBM: the one of the shallow ocean layers that responds rapidly to the atmosphere, the other (greater) of the deeper ocean. The authors suggest that these two different heat capacities are responsible for the fast and slow components observed in the response of their GCM. Our hysteresis experiments, instead, when compared with the Held et al. (2010) approach, are related to a different problem, namely one which does not "return" to a fixed forcing but the forcing is cyclically changed at a given time rate and the transient (not steady) model solutions are followed. Moreover, the EBM discussed here has a single time scale, which is determined by the heat capacity C. This assumption is consistent with the PlaSim solutions shown in Fig. 1a: for any rate of CO_2 change, the relaxation towards equilibrium for CO_2=20 ppm is characterized by a single time scale dictated by the depth of the slab ocean. Thus, the slow component has a different origin in the two cases: in the study by Held et al. (2010) it is related to the slow adjustment of the system towards equilibrium to a sudden reduction of the radiative forcing, while in the present study it is due to the delay of the system in adjusting to the time-dependent forcing variations. The area enclosed by the loop may be a relevant parameter to be considered when greenhouse gases are projected into different future values; the climate, in fact, may be trapped by these loops.

3.2 Global climate model

In this section, we explore whether a similar mechanism holds in the context of a general circulation climate model such as PlaSim. We select one of the rates considered in Section 2 (1.5 ppm $year^{-1}$) and perform a few full cycles varying CO_2 from 360 down to 20 ppm and vice versa. Since the EBM results have been shown in

terms of T_s as a function of the radiative forcing parameter β, we have estimated the radiative forcing change associated with the variation of CO_2 concentration through the simplified expression used in IPCC (Intergovernmental Panel on Climate Change 1990, see also Myhre et al. 1998):

$$\Delta F = 5.35 \cdot \ln\left(\frac{C_{CO2}}{C_0}\right) \tag{5}$$

where C_{CO2} is the CO_2 concentration in parts per million by volume and C_0 is the reference concentration (here set to 360 ppm).

As an example, in Fig. 3a the global mean surface temperature T_s as a function of ΔF is shown both for the ocean depth of 50 m (solid line) and 100 m (dashed line). A single cycle is displayed since additional cycles overlap, apart from the noise introduced by the model interannual variability. As obtained for the EBM (Fig. 2b), the climate model shows a hysteresis cycle related to the memory effect, whose width depends on the depth of the slab ocean. The similarity between the EBM and PlaSim solutions (Figs. 2b and 3a), especially for low values of ΔF, appears evident and robust, at least in the limit of the basic assumptions underlying the EBM (i.e., the threshold on T_s in the planetary albedo change, the representation of the albedo as a step function, the linearization of the outgoing infrared radiation, or the solar radiation assumed to be constant with latitude). Moreover, it is worth noting that for a fixed mixed layer ocean depth and sea ice increasing with decreasing CO_2 from 360 to 20 ppm, one may expect a sea ice-induced change in the ocean heat capacity that would affect the hysteresis cycle. However, it is found that the sea ice contribution to the ocean heat capacity should not change significantly because at 20 ppm the tropics and most of the midlatitudes remain ice-free, and the global mean surface albedo increases from about 0.24 to about 0.4. Thus, this sea ice effect should contribute only marginally to the observed hysteresis cycle that, instead, seems merely controlled by the memory effect and the mixed layer ocean depth.

In complementing the result in Fig. 3a, we show in Fig. 3b, c the global mean surface temperature as a function

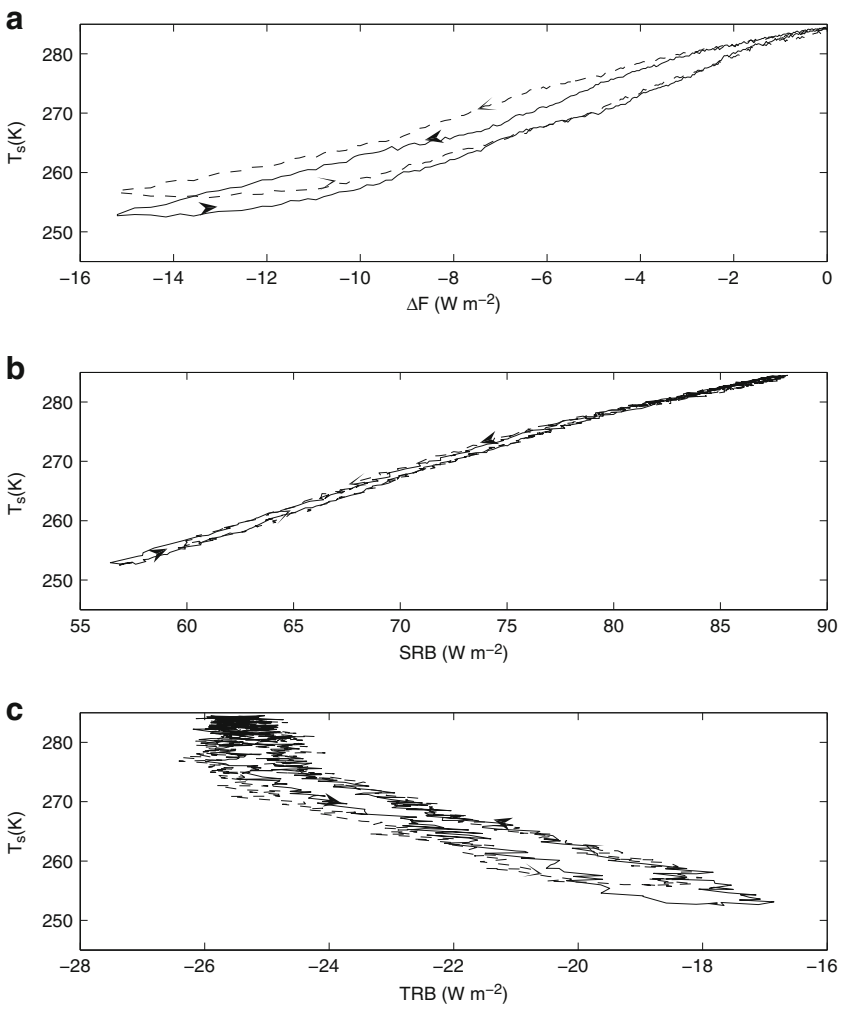

Fig. 3 Hysteresis loops obtained with PlaSim varying back and forth the CO_2 concentration in the range 360–20 ppm at the rate of 1.5 ppm year^{-1} and setting the mixed layer ocean depth equal to 50 m (*solid line*) and 100 m (*dashed line*). Global mean surface temperature T_s (K) as a function of: **a** ΔF (watts per square meter); **b** surface radiation balance (SRB, watts per square meter); and **b** radiation balance at TOA (TRB, watts per square meter). *Arrows* refer to decreasing/increasing CO_2 content. Values of the surface temperature are yearly means

of the net radiation balance at the surface (SRB) and top of the atmosphere (TRB), respectively, which also represent a measure of the radiative forcing. Also in this case, the hysteresis cycles are obtained; however, less similarity is found with Fig. 2b when the ocean depth is varied. It is plausible to think that, while the estimated ΔF well represents the parameter β, SRB and TRB do not because they include all the other effects taken into account by PlaSim, such as those associated with water vapor, ozone, and heat transports.

As a final remark, since in case of memory hysteresis we are dealing with transient climate states far from equilibrium, entropy is not a well-defined quantity and the area enclosed in the loop does not represents the entropy production. The area is a measure of the memory of the model when a time-dependent change of the radiative forcing is applied. On the other hand, as in any hysteresis cycle, the area within the memory loop may be viewed as the work done by the non-conservative forces on the system. In this case, however, the non-conservative forces are difficult to define, certainly they are related to the ocean heat capacity such as the ones involved in the phase change of water or turbulence.

4 Conclusions

The present paper describes the GCM response to a varying greenhouse parameter. It is found that for different time rates of CO_2 change similar transient climates (i.e., characterized by the same global mean surface temperature) can occur for the same value of the greenhouse parameter. Moreover, if we consider a simple energy balance model and cyclically modify the radiative forcing at a given rate within a range that does not include the bifurcation points, a hysteresis occurs which is neither static nor dynamical. The area of the hysteresis loop can be interpreted as a measure of the memory response of the model. A similar response is also obtained by using the global climate model PlaSim. The mechanism here proposed, however, should not be confused with other memory effects that Held et al. (2010) or some of us studied elsewhere (Zhu et al. 2006, 2010). Zhu et al. (2010) studied the long-term memory related to the persistence at a given time scale (Hurst exponent), while Held et al. (2010) isolated the slow component of the global warming by abruptly setting the radiative forcing to its preindustrial value. The two-time scale adjustment discussed by Held et al. (2010) assumed no large hysteresis effects, allowing for a relatively simple description of the short and long time scales involved in the return to preindustrial conditions. Thus, in that paper the return trajectory to climate equilibrium followed (1) the fast adaption of the atmosphere to the new radiative forcing and (2) the slowly interacting sluggish components of the whole system. In the present paper, instead, we have discussed the memory effect of a simple energy balance model and of a global climate model, which have a single time scale determined by the ocean heat capacity, when the radiative forcing is cyclically varied at a given rate from its present value to a value close to the bifurcation point. The memory hysteresis loop so obtained can be related to the lagged response of the system that is unable to relax completely to the equilibria associated with the time-varying forcing values. For a given time rate of CO_2 change, the width of this memory hysteresis loop appears to be controlled by the depth of the passive ocean taken into account by PlaSim. It is plausible to think that if the simulations discussed in Fig. 1a are performed using a coupled atmosphere–ocean GCM, the fast and slow components of the model response towards equilibrium may be distinguished as suggested by Held et al. (2010). In such a case, however, we are dealing with a system mainly driven by the ocean and not by the radiative forcing which we are interested in. Further analyses are envisaged to investigate the role of the full-solved ocean implemented in the current CGMs.

Acknowledgments Support by the Max Planck Society is acknowledged (KF). We thank the two anonymous reviewers for their constructive comments that helped improving the presentation of the paper.

References

Benzi R, Sutera A, Vulpiani A (1981) The mechanism of stochastic resonance. J Phys A: Math Gen 14:L453–L457

Berk A, Bernstein LS, Robertson DC (1989) MODTRAN: a moderate resolution model for LOWTRAN 7, Report GL-TR-89-0122. Air Force Geophys. Lab, Bedford, MA

Bordi I, Dell'Aquila A, Speranza A, Sutera A (2004) On the midlatitude tropopause height and the orographic-baroclinic adjustment theory. Tellus 56A:278–286

Bordi I, Fraedrich K, Lunkeit F, Sutera A (2007) Tropospheric double-jets, meridional cells and eddies: a case study and idealized simulations. Mon Wea Rev 135:3118–3133

Budyko MI (1969) The effect of solar radiation variations on the climate of the Earth. Tellus 21:611–619

Fraedrich K, Lunkeit F (2008) Diagnosing the entropy budget of a climate model. Tellus 60A:921–931

Fraedrich K, Jansen H, Kirk E, Luksch U, Lunkeit F (2005) The planet simulator: towards a user friendly model. Meteorol Zeitschrift 14:299–304

Freidlin MI, Mayergozy ID (2001) Hysteresis in randomly perturbed fast dynamical systems. Physica B 306:15–20

Goldsztein GH, Broner F, Strogatz SH (1997) Dynamical hysteresis without static hysteresis: scaling laws and asymptotic expansions. SIAM J Appl Math 57:1163–1187

Held IM, Winton M, Takahashi K, Delworth T, Zeng F, Vallis GK (2010) Probing the fast and slow components of global warming

by returning abruptly to preindustrial forcing. J Climate 23:2418–2427

Intergovernmental Panel on Climate Change (1990) In: Houghton JT, Jenkins GJ, Ephraums JJ (eds) Climate change: the IPCC scientific assessment. Cambridge University Press, Cambridge, UK

Lucarini V, Fraedrich K, Lunkeit F (2010) Thermodynamic analysis of snowball earth hysteresis experiment: efficiency, entropy production, and irreversibility. Q J R Met Soc 136:2–11

Manabe S, Stouffer RJ, Spelman MJ, Bryan K (1991) Transient response of a coupled ocean–atmosphere model to gradual changes of atmospheric CO2. Part I: annual-mean response. J Climate 4:785–818

Myhre G, Highwood EJ, Shine KP (1998) New estimates of radiative forcing due to well mixed greenhouse gases. Geophys Res Lett 25:2715–2718

Rahmstorf S (1995) Bifurcation of the Atlantic thermohaline circulation in response to changes in the hydrological cycle. Nature 378:145–149

Zhu X, Fraedrich K, Blender R (2006) Variability regimes of simulated Atlantic MOC. Geophys Res Lett 33:L21603

Zhu X, Fraedrich K, Liu Z, Blender R (2010) A demonstration of long term memory and climate predictability. J Climate 23: 5021–5029